Superplastic Behaviour Of Aluminium Alloy - AA5083

Divya H. V, Laxmana Naik L, G. C. Gopalkrishna, V. V. Bongale, Yogesha B
Department of Mechanical Engineering,
Malnad College of Engineering, Hassan, Karnataka, India

Abstract:

In the present investigation experimental and analytical characterization of the high temperature (superplastic) deformation of AA5083 alloy was carried out. Uniaxial tensile test was performed in a temperature range of 748 – 823K at different initial strain rates. Further, a numerical procedure based on MATHEMATICA was developed to predict the tensile response of the alloy for the given deformation condition. Superplasticity is the ability of polycrystalline materials to exhibit, in a relatively uniform/isotropic manner, very large tensile elongations prior to failure, under appropriate conditions of temperature and strain rates. The phenomenon of superplasticity arising due to specific microstructural conditions is commonly referred to as "structural" superplasticity or "micrograin" superplasticity. This behaviour can be utilised in the shaping and forming of parts, components and structures which cannot be easily or economically produced from materials of normally limited ductility.

Keywords*: *Superplasticity, AA5083, MATHEMATICA, ductility, deformation.

1. Introduction:

Superplasticity is the ability of a polycrystalline material to exhibit, in relatively uniform manner, very large elongations prior to failure [Langdon (1982)]. Typically, large elongations are observed at temperatures above 0.5Tm, where Tm is the absolute melting point of the alloy and at a rather limited range of relatively slow strain rates [Padmanabhan et al. (1980) and Pilling et al. (1989)] -see Fig. 1. Elongations in excess of 200% are usually indicative of superplasticity. These materials have very fine grain sizes (usually well below 20μm), which remain stable at the temperature of deformation. The motivation for this study lies on the fact that currently there is a strong interest in the use of superplastic forming technology for the fabrication of automotive sheet parts from 5000 series (i.e., Al-Mg) Aluminium alloys. Of these alloys, AA5083 appears to have the greatest potential for use in automotive applications, but presently being formed by conventional techniques. The behavior of Al-Mg alloys in general and of AA5083 in particular, is not yet fully understood. More investigations on superplastic deformation behaviour as well as formability need to be carried out to use these alloys effectively.

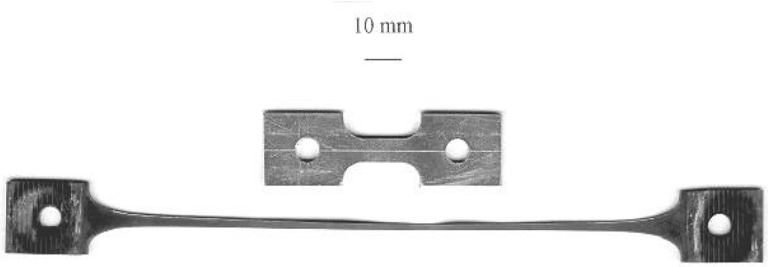

Fig.1. Superplastic deformation of an alloy showing an undeformed (top) and a deformed specimen (bottom).

Superplasticity during tensile deformation arises from a high resistance to the growth of a neck. An indicator of the propensity of a material to resist necking is provided by the strain-rate sensitivity index, m, of the material [Padmanabhan et al. (1980) and Pilling et al. (1989)]. The strain rate sensitivity index is the slope of the double logarithmic stress-strain rate plot, as the stress is related to the strain rate by [Backofen et al. (1964)].

$$\sigma = K\dot{\varepsilon}^{m} \;\Rightarrow\; m\Big|_{\varepsilon,d,T} = \frac{\partial \ln \sigma}{\partial \ln \dot{\varepsilon}}\Big|_{\varepsilon,d,T} \qquad (1)$$

at a constant value of strain (ε), grain size (d) and temperature (T), where σ, $\dot{\varepsilon}$, and m are the true stress, the true strain rate and the strain rate sensitivity index respectively. It is generally accepted that materials with m values of more than 0.3 can be superplastically deformed.

2. Experimental Studies - Superplastic Tensile Behaviour

The Aluminium alloy whose superplastic behavior to be analysed is available in the form of a cold rolled sheet of 1.5 mm thickness. The chemical composition of as-received sheet of the AA5083 alloy obtained using a metals analyser spectrometer and the composition is listed in Table 1.

Microstructural characterisation of the as-received material was carried out using an optical microscope. This was aimed at recording the initial microstructure as well as the grain size of the alloy. The sample were prepared by following standard procedures of mechanical polishing on a series of emery papers followed by diamond polishing and finally etching with Keller's reagent (6ml HBF4 + 26ml HCl + 48ml HNO3). The 2D grain size was determined by using the linear intercept method in both the longitudinal and transverse directions of the rolled sheet.

Table 1 Chemical composition of the AA5083 alloy.

Element	Al	Mg	Mn	Fe	Si	Cr	Ti	Zn	Pb
Weight %	92.86	5.40	0.90	0.36	0.15	0.114	0.026	0.048	0.01

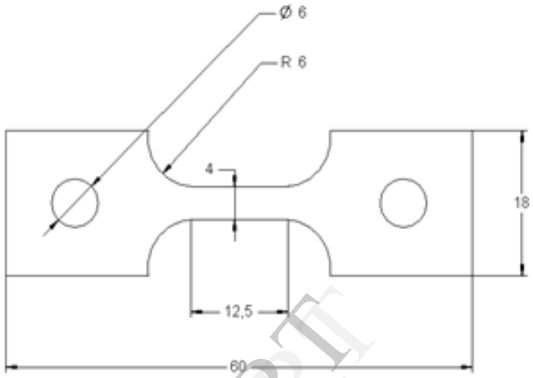

All Dimensions in mm. (Not to scale)
Fig.2 High temperature tensile test sample

Test specimen was machined directly from the as received sheet with its tensile axis parallel to the rolling direction. The tensile specimen had a gauge length of 12.5mm and a gauge width of 4 mm and thickness of 1.5mm as shown in Fig.2. Prior to testing, the specimen was mechanically polished to remove fine scratches from the specimen surface, particularly in the gauge portion.

2.1 Tensile Testing Equipment:

For the high temperature uniaxial tensile testing campaign, a microprocessor controlled electro-mechanical screw driven testing machine (SCHENCK TREBEL) of 250kN capacity was used. The machine is direct current driven with facilities for conducting constant cross head speed control, force control and strain control tests. For the measurement and control of the cross head displacement, the machine is provided with data acquisition and control system. For the measurement of static and dynamic tensile and compressive forces load cells of 1kN, 10kN and 250kN capacity, based on ring torsion principle, are provided. For isothermal conditions of testing the machine has a thyristor controlled two zone split furnace which ensures that a uniform temperature zone of about 300mm can be maintained up to 1200°C with an accuracy of ± 3°C. The feed

back for the temperature controller is obtained from three Pt-Pt 10% Rh thermocouples placed in the two zones. In this study the load was measured using a 1kN load cell. Fig.3 shows a schematic drawing of the set-up used for the high temperature tensile tests.

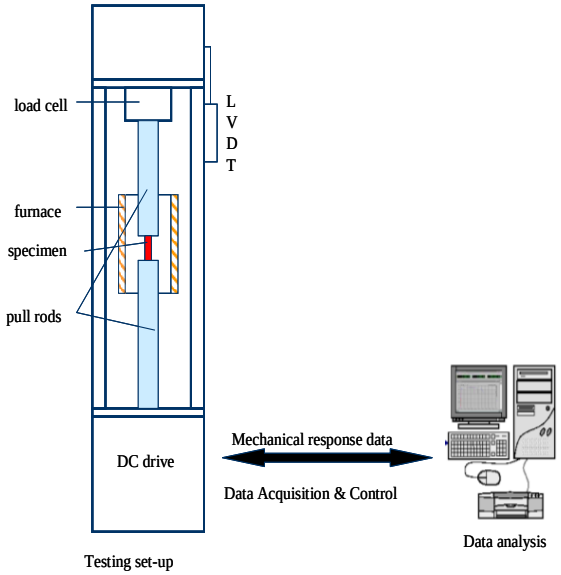

Fig. 3 Schematic drawing of the experimental set-up

2.2 Testing Procedure:

For all the tests, the furnace was switched on first and the sample is loaded only after the furnace had reached the test temperature. This precaution was necessary to reduce the exposure time at high temperatures and, thereby, reduce grain growth and oxidation (in case of alloys that are prone to oxidation). After the specimen was loaded and the furnace was closed, about 10 minutes were allowed for the temperature to stabilise under a small constant tensile load (in order to offset the thermal expansion of the system which would otherwise lead to the buckling of the specimen due to compression). After the temperature stabilised in the furnace, the machine was switched from “force control” to “displacement control” and the specimen was subjected to tensile loading under a constant displacement (constant cross head speed) rate up to failure. The displacement position was reset to zero just before the commencement of the test and the initial dimensions (gauge length, width and thickness) were entered into the display panel for storage. The data acquisition software programme was activated then and the data obtained in a digital format.

3. Results and Discussions:

From the load elongation test data, the standard tensile properties (ultimate strength and percent elongation prior to failure) were evaluated. Table 2 gives the percent elongation to failure and the Ultimate Tensile Strength (UTS) obtained in the alloy at different test

conditions. From the data it can be seen that the alloy exhibited reasonably good tensile elongations (more than 190%) in most of the cases.

Fig. 4 shows the strain hardening characteristics (in terms of true stress-true strain plots) of the specimen tested at different initial strain rates and temperature. In general the alloy showed an increase in strain to failure with an increase in initial strain. Further, the slope of the stress strain curve also decreased with the decreasing initial strain rate, thereby the delaying the attainment of maximum stress before failure in the alloy. Extensive strain hardening took place initially and after reaching maximum, the flow stress decreased continuously until fracture. At higher deformation rates the strain hardening rate saturated early during deformation, whereas the early deformation rates showed a more sustained hardening rate maintained to higher strain levels.

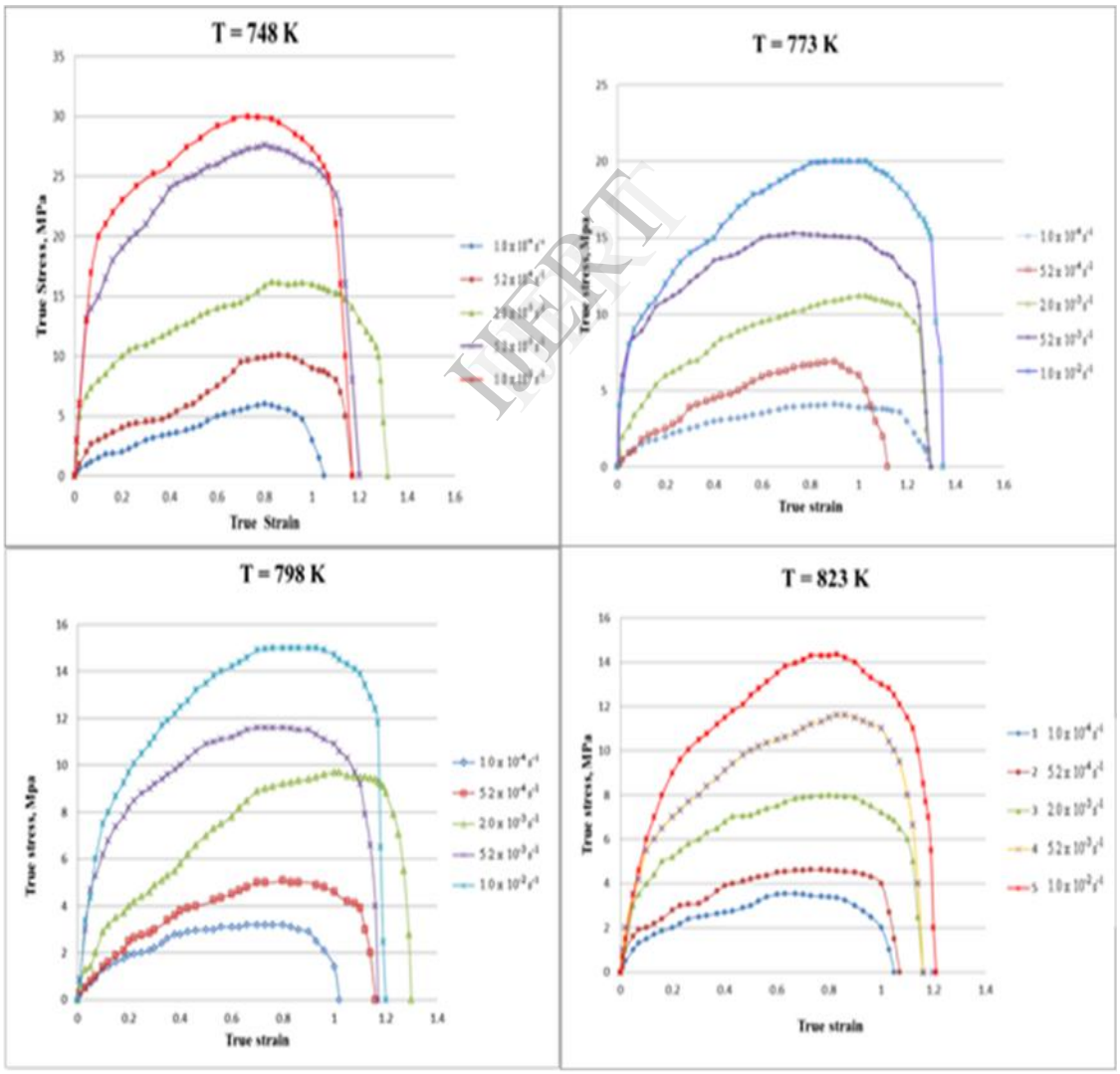

Fig. 4 Effect of the variation of initial strain rate on the true stress-strain behavior from 748K - 823 K

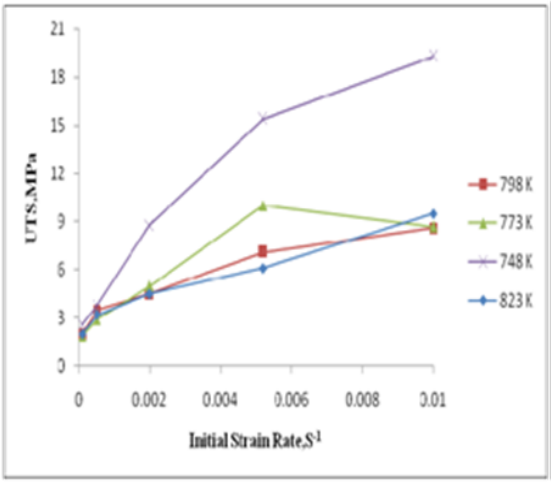

Fig. 5 Variation of UTS with initial strain rate at different temperatures.

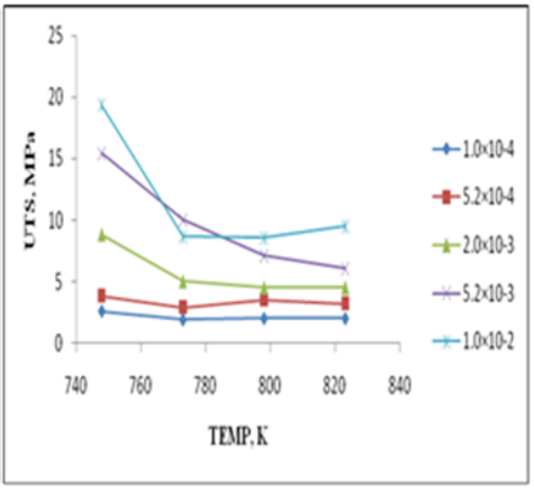

Fig. 6 Variation of UTS with temperatures at different initial strain rate

Table 2 High temperature mechanical properties for the alloy at different conditions of testing

Temperature (K)	Strain Rate, s^{-1}	UTS, MPa	Elongation to Failure, %
823	1.0×10^{-4}	2	185
	5.2×10^{-4}	3.2	193
	2.0×10^{-3}	4.5	211
	5.2×10^{-3}	6.1	209
	1.0×10^{-2}	9.5	236
798	1.0×10^{-4}	2	180
	5.2×10^{-4}	3.5	221
	2.0×10^{-3}	4.5	270
	5.2×10^{-3}	7.1	220
	1.0×10^{-2}	8.6	234
773	1.0×10^{-4}	1.9	256
	5.2×10^{-4}	2.9	210
	2.0×10^{-3}	5	265
	5.2×10^{-3}	10	280
	1.0×10^{-2}	8.7	262
748	1.0×10^{-4}	2.6	188
	5.2×10^{-4}	3.8	215
	2.0×10^{-3}	8.8	270
	5.2×10^{-3}	15.4	232
	1.0×10^{-2}	19.3	218

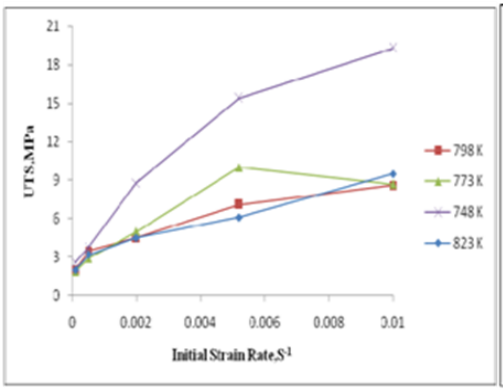

Fig. 5 Variation of UTS with initial strain rate at different temperatures.

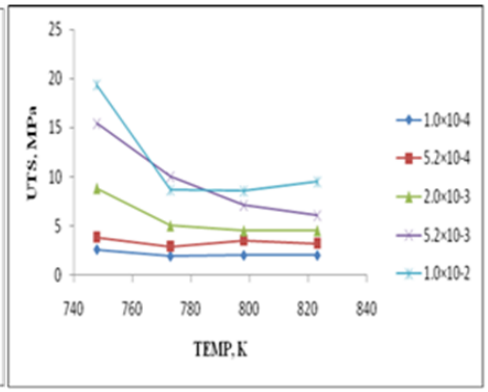

Fig. 6 Variation of UTS with temperatures at different initial strain rate

Fig.5 shows the variation of the UTS with initial strain rate at different temperatures and Fig.6 shows the variation of the UTS with temperature at different initial strain rates. The UTS decreased as the temperature increased at an initial strain rate of deformation, and at a fixed temperature level the UTS increased with increasing strain rate. Strain softening following a stress maximum occurred until failure and roughly uniform deformation took place within the gauge length and the steady state flow stress was observed at all examined temperatures in the alloy. Results show the sample exhibited superior tensile ductility. Final necking leading to fracture was observed.

At high strain rates, the hardening component was essentially due to dislocation process such as pile-ups, tangles and sub-grain formations, which at the higher temperatures, saturated very quickly [Verma *et al.*, 1995]. At a lower strain rate of $5.2\times10^{-4}s^{-1}$, the deformation was almost entirely in the optimal superplastic deformation regime.

3.1 Prediction of Tensile Behaviour Using Statistical Package like MATHEMATICA

The current problem is concerned with the prediction of the process parameters in case of the superplastic tensile test of aluminium alloy. Aluminium alloy such as AA5083 find extensive use in aerospace applications. However, performing the experiment all the time to assess the forming characteristics is a tedious and costly process. This part mainly deals with the formulation of the experimental data.

The data required for performing the regression analysis in case of high temperature tensile test of Aluminium is from the experiment itself. The tensile test was carried on the Aluminium alloy and the process characteristics such as maximum yield stress and percent elongation was measured on the temperature and strain rate.

The multiple programmatic regression analysis was carried out using MATHEMATICA. The experimental Temperature and Strain Rate were taken as the predictors and the corresponding UTS (MPa) and percent elongation were taken as the responses at a time. Fig.7 and 9 shows the comparison between the experimental and the predicted responses

resulted from the multiple regressions using MATHEMATICA. Fig.8 and 10 shows the relative error between the experimental and the predicted responses. The relative error was calculated by using the formula:

$$\text{Relative Error} = \frac{\ln(\text{Predicted}) - \ln(\text{Experimental})}{\ln(\text{Experimental})} \times 100\% \qquad (2)$$

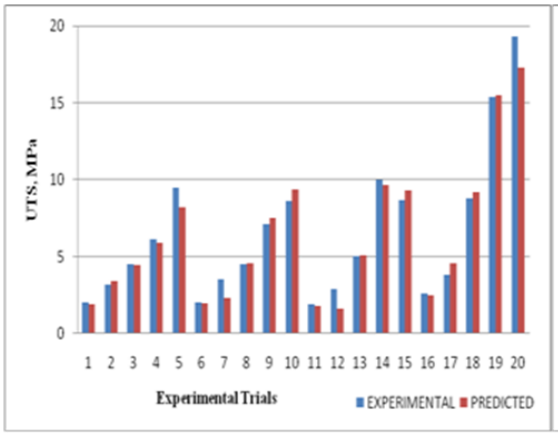

Fig. 7 Comparison between the experimental and predicted UTS (MPa)

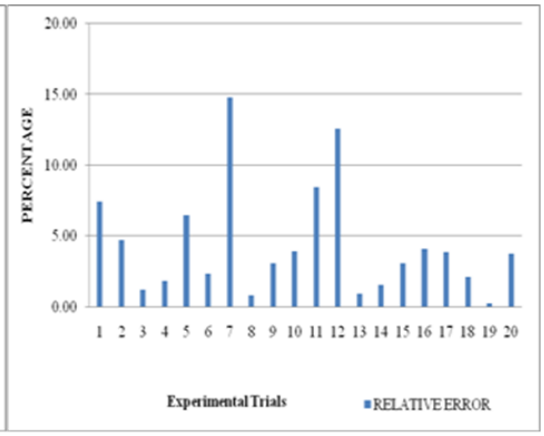

Fig. 8 Relative error between the experimental and predicted UTS (MPa)

It can be observed that the predicted responses are in good agreement with the experimental results and the percent relative errors are less than 10%. The predictions by MATHEMATICA were in reasonable agreement with experimentally observed results. The minimum error of 0.23 found at the temperature of 748K and ISR 5.2×10-3 s^{-1}. The maximum error of 14.80 is found at the temperature of 798K and ISR 5.2×10-4 s^{-1}. It can be observed that the predicted responses are in good agreement with the experimental results and the percent relative errors are less than 10%.

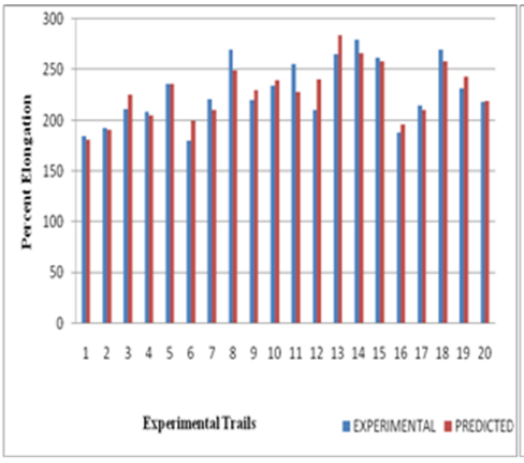

Fig. 9 Comparison between the experimental and predicted percent elongation

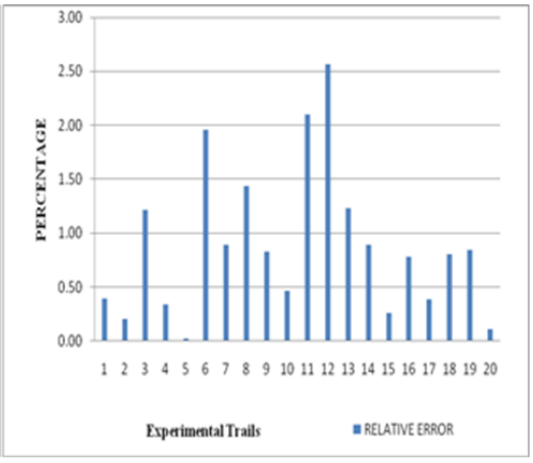

Fig. 10 Relative error between the experimental and predicted percent elongation

4. Conclusions:

In the present investigation experimental and analytical characterization of the high temperature (superplastic) deformation of AA5083 alloy was carried out. Uniaxial tensile test was performed in a temperature range of 748 – 823K at different initial strain rates. Further, a numerical procedure based on MATHEMATICA was developed to predict the tensile response of the alloy for the given deformation condition.

The following major conclusions could be drawn:

1. Elongations to failure of more than about 190% were observed in most of the cases. A maximum elongation of 280% at 773 K and 5.2×10^{-3} s^{-1} was observed.
2. The optimal superplastic temperature and strain rate ranges were found to be 773 - 798 K and 5.2×10^{-4} to $2.0 \times 10^{-3} s^{-1}$ for the alloy selected.
3. The numerical model based on regression analysis using MATHEMATICA for the prediction of the tensile behaviour of the alloy studied could accurately predict the stresses for the given deformation conditions (temperature, strain rate, strain), well within the limits of experimental error (0.02 to 14%).

References:

1. Backofen W.A., I.R. Turner and D.H. Avery (1964), Superplasticity in an Al-Zn Alloy, Trans. ASM, 57, 980-990.
2. Davies, C.J., J.W. Edington, C.P. Cutler, and K.A. Padmanabhan (1970) Superplasticity: A Review. Journal of Material Science, 5, 1091-1102
3. Edington, J.W., K.N. Melton and C.P. Cutler (1976), Superplasticity Prog. Mater. Sci., 21, 61-170
4. Langdon T. G. (1982), Metallurgical Transactions. 13A, 689-701.
5. Padmanabhan, K.A (1977), A Theory of Structural Superplasticity. Material Science. Eng, 29, 1-18.
6. Padmanabhan, K.A and G.J. Davies Superplasticity. Springer-Verlang, Berlin, 1980
7. Pilling, J and N. Ridley Superplasticity in Crystalline solids" Institute of Metals, 1989.
8. Sherby O.D. and J. Wadsworth (1985), Overview: Superplasticity and superplastic forming processes, Material Science and Technology, 1, 925-936.
9. Verma R., A.K. Ghosh, S.Kim and C.Kim (1995), Grain refinement and superplasticity in 5083 Al, Materials Science and Engineering, A, 191 (1-2), 143-150.
10. Yogesha .B and Bhattacharya .S .S, Superplastic Behaviour of a Ti-Al-Mn Alloy, International Journal for Manufacturing Science & Production Vol. 9, Nos. 1-2, 2008.